

Pseudogap phase in cuprates: oxygen orbital moments instead of circulating currents

A. S. Moskvin¹⁾

Department of Theoretical Physics, Ural Federal University, 620083 Ekaterinburg, Russia

Submitted 3 August 2012

Circulating current (CC) loops within the cuprate unit cell are proposed to play a key role in the physics of the pseudogap phase. However, main experimental observations motivated by this sophisticated proposal and seemingly supporting the CC model can be explained in frames of a simple and physically clear microscopic model. We argue that instead of a well-isolated Zhang–Rice (ZR) singlet $^1A_{1g}$ the ground state of the hole center $[\text{CuO}_4]^{5-}$ (cluster analog of Cu^{3+} ion) in cuprates should be described by a complex $^1A_{1g}^{-1,3}B_{2g}^{-1,3}E_u$ multiplet, formed by a competition of conventional hybrid Cu $3d$ -O $2p$ $b_{1g}(\sigma) \propto d_{x^2-y^2}$ state and *purely oxygen nonbonding* O $2p\pi$ states with $a_{2g}(\pi)$ and $e_{u_{x,y}}(\pi)$ symmetry. In contrast with inactive ZR singlet we arrive at several novel competing orbital and spin-orbital order parameters, e.g., Ising-like net orbital magnetic moment, orbital toroidal moment, intra-plaquette's staggered order of Ising-like oxygen orbital magnetic moments. As a most impressive validation of the non-ZR model we explain fascinating results of recent neutron scattering measurements that revealed novel type of magnetic ordering in pseudogap phase of several hole-doped cuprates.

Introduction. The nature of the pseudogap (PG) phase to be the most puzzling and anomalous region of the phase diagram of the cuprate high-temperature superconductors is one of major unsolved problems in condensed matter physics. Different theoretical models describe the pseudogap state as a precursor of the superconducting d -wave gap with preformed pairs below T^* which would acquire phase coherence below T_c or a phase competing with the superconducting one that ends at a quantum critical point, typically inside the superconducting dome. The order parameter associated with these competing phases may involve charge and spin density waves or charge currents flowing around the CuO_2 square lattice, such as D -charge density wave or orbital circulating currents (see, e.g., Ref. [1] for a short overview). In his theory for cuprates, C. M. Varma [2] proposes that PG is a new state of matter associated with the spontaneous appearance of circulating current (CC) loops within CuO_2 unit cell. The current pattern is assumed to disappear only at a quantum critical point at a hole doping level of $x_c \sim 0.19$. This Intra-Unit-Cell (IUC) order breaks time reversal symmetry (TRS), but preserves lattice translation invariance. From a theoretical point of view the existence of a CC-loop order and the ability of such a $q = 0$ instability to produce a gap in the charge excitation spectrum are still highly controversial [3, 4]. However, several experimental observations motivated by this proposal pointed to a symmetry breaking in the pseudo-gap phase [5–9] and provided strong encouragement for models based on CC-loop or-

der in copper oxide materials. The TRS violation in the PG state of Bi2212 was first inferred from the observation of dichroic effect in ARPES measurements [5], but this measurement has been the subject to a long standing controversy (see, e.g., Ref. [10]).

Seemingly the strongest experimental evidence for an orbital-current phase are the observations of an unusual translational-symmetry preserving magnetic order in underdoped $\text{YBa}_2\text{Cu}_3\text{O}_{6+x}$, $\text{HgBa}_2\text{CuO}_{4+\delta}$, $\text{La}_{2-x}\text{Sr}_x\text{CuO}_4$, and $\text{Bi}_2\text{Sr}_2\text{CaCu}_2\text{O}_{8+\delta}$ by spin-polarized neutron diffraction [6, 8]. However, local probes of magnetism, such as nuclear magnetic resonance (NMR) and zero-field muon spin relaxation (ZF- μ SR) have found no evidence for the onset of magnetic order at the pseudogap temperature T^* [11–13]. Very recent high-precision ZF- μ SR measurements of $\text{La}_{2-x}\text{Sr}_x\text{CuO}_4$ in the Sr concentration (hole-doping) range $0.13 < x < 0.19$ [13] do not support theoretically predicted loop-current phases [2], and point to an alternative explanation for the unusual magnetic order detected by spin-polarized neutron diffraction at lower hole doping. Hereafter in this Letter we address such an alternative scenario.

Non-Zhang-Rice model and order parameters. The problem of the order parameters in hole doped cuprates is closely related to that of ground state of the hole centers CuO_4^{5-} to be cluster analogues of the Cu^{3+} ion. The nature of the doped-hole state in the cuprates with nominally Cu^{2+} ions such as La_2CuO_4 is a matter of great importance in understanding both the mechanism leading to the high-temperature superconductivity and unconventional normal state behavior of

¹⁾ e-mail: alexandr.moskvin@usu.ru

the cuprates. In 1988 Zhang and Rice [14] have proposed that the doped hole forms a well isolated local spin and orbital ${}^1A_{1g}$ singlet state which involves a phase coherent combination of the $2p\sigma$ orbitals of the four nearest neighbor oxygens with the same b_{1g} symmetry as for a bare Cu $3d_{x^2-y^2}$ hole. This all assumes that, in the low energy limit, the Cu–O system can be reduced to an effective single orbital, or one-band model.

However, numerous experimental data, in particular, recent magnetic neutron scattering findings (see review article Ref. [6]), suggests the involvement of some other physics which introduces low-lying states into the excitation of the doped-hole state, or competition of conventional Zhang–Rice (ZR) state with another electron removal state. This point was discussed earlier, however, mainly as an interplay between ZR singlet ${}^1A_{1g}$ and triplet ${}^3B_{1g}$, formed by additional hole going not into b_{1g} state as in ZR singlet, but into $a_{1g} \propto d_{z^2}$ state [15]. It is worth noting that ${}^3B_{1g}$ state corresponds to a Hund ${}^3A_{2g}$ term of two-hole e_g^2 configuration of an undistorted CuO_6 octahedra. However, later experimental findings for very different insulating cuprates and theoretical calculations have shown that the energy separation between the $b_{1g}(d_{x^2-y^2})$ and $a_{1g}(d_{z^2})$ orbitals in CuO_4 plaquettes is thought to be of the order of 1.5 eV, i.e. too large for quasi-degeneracy and effective vibronic coupling. More sophisticated version of the non-ZR states was proposed by Varma [2], who has proposed that the additional holes doped in the CuO_2 planes do not hybridize into ZR singlets, but give rise to circulating currents on O–Cu–O triangles.

On the other hand, cluster model considerations supported by numerous experimental data point to a competition of conventional hybrid Cu $3d$ -O $2p$ $b_{1g}(\sigma) \propto d_{x^2-y^2}$ state with purely oxygen nonbonding O $2p\pi$ states with $a_{2g}(\pi)$ and $e_{ux,y}(\pi) \propto p_{x,y}$ symmetry (see Refs. [16, 17] and references therein). Accordingly, the ground state of such a non-ZR hole CuO_4^{5-} center as a cluster analog of Cu^{3+} ion should be described by a complex ${}^1A_{1g}$ - ${}^3B_{2g}$ - 3E_u valence multiplet with several order parameters such as spin and Ising-like orbital magnetic moments, dipole and quadrupole electric moments prone to strong vibronic coupling, and more subtle hidden order parameters.

Earlier we have addressed unconventional properties of the non-ZR hole center related to the ${}^1A_{1g}$ - 3E_u quasi-degeneracy (A–E model) [16]. Fig. 1 shows the term structure of the actual valence A–E multiplet together with single-hole basis b_{1g}^b ($|b_{1g}\rangle = c_d|d_{x^2-y^2}\rangle + c_p|b_{1g}(\text{O}2p)\rangle$) and $e_{ux,y}$ ($|e_{ux,y}\rangle = c_\pi|e_{ux,y}(\pi)\rangle + c_\sigma|e_{ux,y}(\sigma)\rangle$) orbitals. The e_u orbitals could form two circular current $p_{\pm 1}$ -like states, $e_{u\pm 1}$ with an Ising-

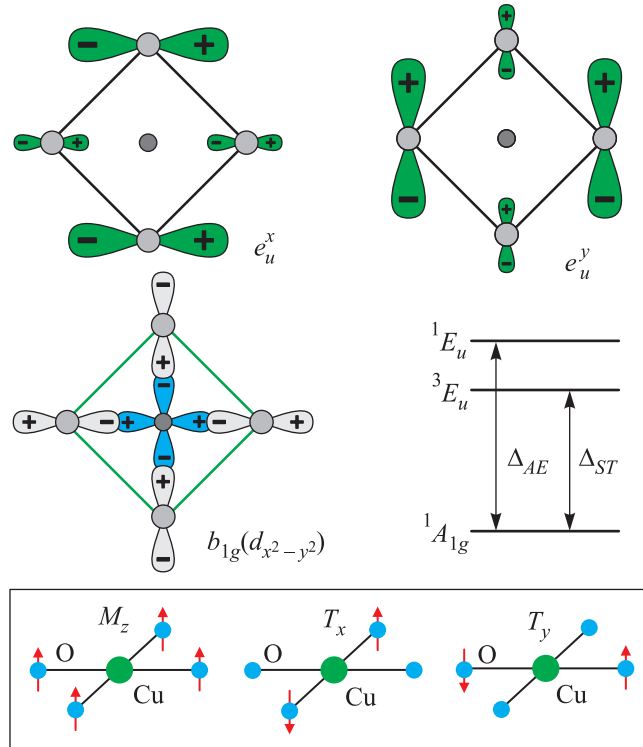


Fig. 1. (Color online) The term structure of the actual valence A–E multiplet for a hole CuO_4^{5-} center together with the single-hole b_{1g}^b and $e_{ux,y}^b$ orbitals. Lower panel illustrates the ferromagnetic and toroidal orderings of the oxygen orbital magnetic moments within the CuO_4 plaquette

like orbital moment $\langle e_{u\pm 1} | l_z | e_{u\pm 1} \rangle = \pm 2c_\sigma c_\pi$ which is easily prone to be quenched by a low-symmetry crystal field with formation of two currentless, e.g., $p_{x,y}$ -like $e_{ux,y}$ states. Even with neglecting the spin degree of freedom we arrive at the eight order parameters for the hole $[\text{CuO}_4]^{5-}$ center including both conventional (two-component in-plane electric dipole moment, three-component in-plane electric quadrupole moment) and unconventional (Ising-like purely oxygen orbital magnetic moment and two-component in-plane purely oxygen orbital toroidal moment) ones (see Fig. 1). Thus, the CuO_4 plaquette with $({}^1A_{1g}, {}^1E_u)$ valent multiplet forms an unconventional magneto-electric center characterized by eight independent orbital order parameters. Even this simplified model predicts broken time-reversal (T) symmetry, two-dimensional parity (P), and basic tetragonal (four-fold Z_4) symmetry. The situation seems to be more involved, if we take into account spin degree of freedom, in particular, the ${}^1A_{1g}$ - 3E_u singlet-triplet mixing effects. First of all, such a center is characterized by a true spin $S = 1$ moment being gapped, if the ZR singlet ${}^1A_{1g}$ has the lowest energy. Strictly speaking, for

our two hole configuration we should introduce two spin operators: net spin moment $\hat{\mathbf{S}} = \hat{\mathbf{s}}_1 + \hat{\mathbf{s}}_2$ and spin operator $\hat{\mathbf{V}} = \hat{\mathbf{s}}_1 - \hat{\mathbf{s}}_2$ that changes spin multiplicity. It should be noted that the V -type order implies an indefinite ground state spin multiplicity and at variance with S -type order is invariably accompanied by an orbital order. The singlet-triplet structure of the $A-E$ multiplet implies two novel types of the spin-orbital order parameters: spin-dipole parameters $\langle \hat{\mathbf{V}} \hat{d}_x \rangle$ and $\langle \hat{\mathbf{V}} \hat{d}_y \rangle$ and spin-toroidal parameters $\langle \hat{\mathbf{V}} \hat{T}_x \rangle$ and $\langle \hat{\mathbf{V}} \hat{T}_y \rangle$. Novel ordering does not imply independent V -, d - or T -type orders.

Despite a “fragility” of the orbital e_u -currents with regard to a crystal field quenching these can produce ferromagnetic-like fluctuations that can explain numerous manifestations of a weak ferromagnetism in different cuprates (see, e.g., Ref. [18]) and a remarkable observation of a weak magnetic circular dichroism (MCD) in $\text{YBa}_2\text{Cu}_3\text{O}_{6+x}$ [7]. It should be noted that the value of MCD effect does not straightforwardly depends on the value of orbital, or magnetic orbital moment. Generally speaking, the hole doped cuprate could be a system with a giant circular magneto-optics if we were able to realize the uniform ferromagnetic ordering of the orbital e_u -currents. It seems likely that the relative concentration $x_h \sim 10^{-4}$ of circularly polarized e_u holes is enough to provide the same magnitude of MCD as an applied magnetic field of 1 Tesla. It is worth noting that the current loop state [2], by itself, is incompatible with ferromagnetism and cannot explain the Kerr measurements [7].

It is worth noting that occurrence of both orbital toroidal and spin-dipole order parameters point to the hole CuO_4^{5-} centers as polar centers with effective magneto-electric coupling which can provide ferroelectric and magnetoelectric properties for hole-doped cuprates [19]. Interestingly, within the ${}^1A_{1g}, {}^1E_u$ multiplet the electric dipole moment operator can be coupled with orbital toroidal and magnetic moments by a remarkable magnetoelectric relation [16, 17]: $\hat{d}_x = d_{me} \{ \hat{T}_y, \hat{M}_z \}$, $\hat{d}_y = -d_{me} \{ \hat{T}_x, \hat{M}_z \}$.

Hereafter we address novel effects related with the ${}^1A_{1g} - {}^1,3B_{2g}$ quasi-degeneracy ($A-B$ -model). Unconventional orbital $A-B$ structure of the hole CuO_4 hole centers with the ground state $b_{1g}^2: {}^1A_{1g} - b_{1g}a_{2g}(\pi): {}^1,3B_{2g}$ multiplet (see Fig. 2) implies several spin, charge, and orbital order parameters missed in the simple ZR model. For the orbital quasi-doublet ${}^1A_{1g} - {}^1B_{2g}$ to be properly described one might make use of a pseudo-spin formalism with two states ${}^1A_{1g}$ and ${}^1B_{2g}$ attributed to $|+1/2\rangle$ and $|-1/2\rangle$ states of a pseudo-spin $s = 1/2$, respectively. Then we introduce three order parameters: $\langle \hat{\sigma}_z \rangle$, $\langle \hat{\sigma}_x \rangle$, and $\langle \hat{\sigma}_y \rangle$, where $\hat{\sigma}_i$ is Pauli matrix. Order param-

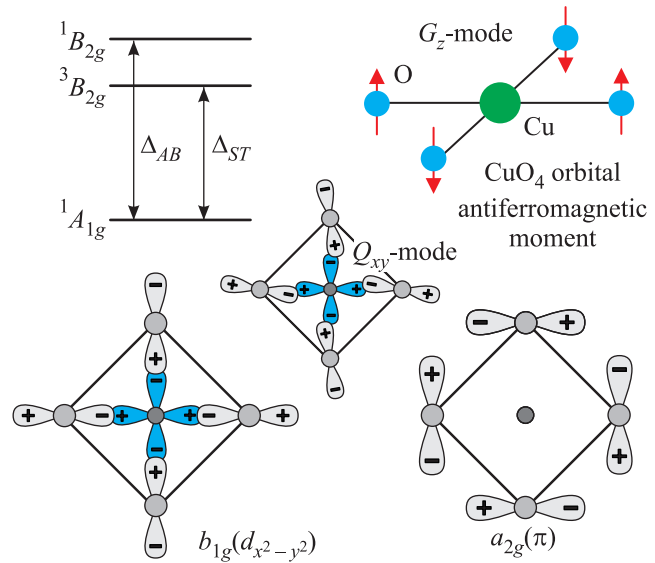


Fig. 2. (Color online) The term structure of the actual valent $A-B$ multiplet for hole CuO_4^{5-} center together with single-hole basis b_{1g}^b and a_{2g}^b orbitals. Shown are antiferromagnetic (staggered) ordering of oxygen orbital magnetic moments within CuO_4 plaquette (G_z -mode) and quadrupole Q_{xy} -mode

eter $\langle \hat{\sigma}_z \rangle$ defines the symmetry conserving charge density fluctuations within the CuO_4 plaquette: Order parameter $\langle \hat{\sigma}_x \rangle$ defines electric quadrupole moment of B_{2g} symmetry localized on four oxygen sites:

$$Q_{xy} = \sum_i \hat{Q}_{xy}(i) = Q_{B_{2g}} \langle \hat{\sigma}_x \rangle. \quad (1)$$

It should be emphasized that the quadrupole moment has an electronic orbital origin (see Fig. 2) and has nothing to do with any CuO_4 plaquette’s distortions or charge imbalance between the density of holes at the oxygen sites. It is worth noting that usually a spontaneous imbalance between the density of holes at the oxygen sites in the unit cell is related to a so-called *nematic* order. Order parameter $\langle \hat{\sigma}_y \rangle$ defines an antiferromagnetic (staggered) ordering of oxygen orbital moments localized on four oxygen sites:

$$\langle \hat{G}_z \rangle = \langle \hat{l}_{1z} - \hat{l}_{2z} + \hat{l}_{3z} - \hat{l}_{4z} \rangle = g_L \langle \hat{\sigma}_y \rangle, \quad (2)$$

where $g_L \approx -1.0$, if to make use of estimates of the cluster model [17]. In other words, maximal value of antiferromagnetic order parameter G_z corresponds to a staggered order of unexpectedly large oxygen orbital magnetic moments $m_z \approx 0.25 \beta_e$. In contrast with the net orbital moment M_z the G_z order cannot be easily quenched by low-symmetry crystal fields. Fig. 2 shows an illustration of the G_z order in the CuO_4 plaquette. In fact, both quadrupole moment $Q_{B_{2g}}$ and local anti-

ferromagnetic ordering of oxygen orbital moments G_z do result from the ${}^1A_{1g}$ - ${}^3B_{2g}$ mixing effect, in other words, these are a result of the symmetry breaking. It should be emphasized that the G_z order resembles the hotly discussed order of circulating currents, proposed by Varma [2].

Two unconventional vectorial order parameters are associated with the ${}^1A_{1g}$ - ${}^3B_{2g}$ singlet-triplet mixing effect: $\langle \hat{V}\hat{Q}_{xy} \rangle$ and $\langle \hat{V}\hat{G}_z \rangle$. It should be noted that corresponding orderings do not imply independent $\langle \hat{V} \rangle$, $\langle \hat{Q}_{xy} \rangle$ or $\langle \hat{G}_z \rangle$ orders. Moreover, the $\langle \hat{V}\hat{Q}_{xy} \rangle$ and $\langle \hat{V}\hat{G}_z \rangle$ orders imply all the mean values $\langle \hat{S} \rangle$, $\langle \hat{V} \rangle$, $\langle \hat{Q}_{xy} \rangle$, $\langle \hat{G}_z \rangle$ for CuO_4^{5-} center together with their on-site counterparts such as $\langle \hat{S}_i \rangle$, $\langle \hat{Q}_{xy}(i) \rangle$, $\langle \hat{l}_{iz} \rangle$ ($i = \text{Cu}, \text{O}_{1,2,3,4}$) turn into zero, at least in first order on the ${}^1A_{1g}$ - ${}^3B_{2g}$ mixing parameters. All novel orbital and spin-orbital order parameters appear to be strongly hidden, or the hard-to-detect ones and can be revealed only by specific experimental technique, for instance, by magnetic polarized neutron diffraction.

Novel orbital modes as seen by neutron diffraction. Matrix element of the spin interaction of a neutron with a CuO_4^{5-} center can be written as follows [20]:

$$\langle SM_S\Gamma\mu | \hat{V}_{\mathbf{pp}'} | S'M_S'\Gamma'\mu' \rangle = -\frac{4\pi\hbar^2}{m} r_0\gamma \times \\ \times \langle SM_S\Gamma\mu | \sum_{\nu} \hat{s}_{\nu} e^{i\mathbf{q}\mathbf{r}_{\nu}} | S'M_S'\Gamma'\mu' \rangle [\mathbf{S}_n - (\mathbf{e}\mathbf{S}_n)\mathbf{e}], \quad (3)$$

where sum runs on the two holes ($\nu = 1, 2$); $\mathbf{s}_{l\nu}$ is the hole spin; $\mathbf{e} = \mathbf{q}/q$ – a unit scattering vector; r_0 – electromagnetic electron radius; $\gamma = -1.913$ – neutron magnetic moment in nuclear Bohr magnetons. Introducing S - V representation we make a replacement for the spin magnetic amplitude:

$$\sum_{\nu} \hat{s}_{\nu} e^{i\mathbf{q}\mathbf{r}_{\nu}} = \frac{1}{2} \hat{S}(e^{i\mathbf{q}\mathbf{r}_1} + e^{i\mathbf{q}\mathbf{r}_2}) + \frac{1}{2} \hat{V}(e^{i\mathbf{q}\mathbf{r}_1} - e^{i\mathbf{q}\mathbf{r}_2}) = \\ = \hat{S}\hat{f}_S(\mathbf{q}) + \hat{V}\hat{f}_V(\mathbf{q}). \quad (4)$$

In other words, we introduce the S - and V -type spin-orbital operators for CuO_4^{5-} centers with corresponding order parameters which can be detected by polarized neutrons. As well as spin operator \hat{V} changes spin multiplicity, the $\hat{f}_V(\mathbf{q})$ operator changes orbital state. For nonzero orbital matrix elements neglecting two-site integrals we obtain

$$\langle {}^1A_{1g} | \hat{f}_V(\mathbf{q}) | {}^3B_{2g} \rangle = -\frac{gL}{4} (\cos q_x l + \cos q_y l) \langle p_x | e^{i\mathbf{q}\mathbf{r}} | p_y \rangle; \quad (5)$$

$$\langle {}^1A_{1g} | \hat{f}_V(\mathbf{q}) | {}^3E_{u,x,y} \rangle = \mp \frac{igL}{2\sqrt{2}} (c_{\pi} \sin q_{y,x} l \langle p_{y,x} | e^{i\mathbf{q}\mathbf{r}} | p_{x,y} \rangle -$$

$$-c_{\sigma} \sin q_{x,y} l \langle p_{x,y} | e^{i\mathbf{q}\mathbf{r}} | p_{x,y} \rangle); \quad (6)$$

$$\langle p_{x,y} | e^{i\mathbf{q}\mathbf{r}} | p_{y,x} \rangle = -3 \langle j_2(qr) \rangle_{2p} e_x e_y, \quad (7)$$

$$\langle p_{x,y} | e^{i\mathbf{q}\mathbf{r}} | p_{x,y} \rangle = \langle j_0(qr) \rangle_{2p} - \frac{3}{2} \langle j_2(qr) \rangle_{2p} (e_{x,y}^2 - e_{y,x}^2), \quad (8)$$

where $\langle j_l(qr) \rangle_{2p}$ is a radial average of spherical Bessel function, $l = R_{\text{CuO}} = a/2$, the “-” and “+” signs are assigned to matrix elements with E_{ux} and E_{uy} , respectively. It should be noted that at $\mathbf{q} = 0$: $\hat{f}_S(0) = 1$, $\hat{f}_V(0) = 0$.

Matrix element for the coupling of the neutron spin with the electron orbital moment can be written as (3), if the spin operator (4) to replace by an effective \mathbf{q} -dependent orbital operator as follows [20]

$$\hat{\Lambda}(\mathbf{q}) = \frac{1}{4} \sum_{n=1}^4 \sum_{\nu} \left\{ \hat{l}_{n\nu}, f(\mathbf{q} \cdot \mathbf{r}_{n\nu}) \right\} e^{i\mathbf{q}\mathbf{R}_n}, \quad (9)$$

where $\hat{l}_{n\nu}$ is the orbital moment operator for ν -hole on the n -th oxygen site, n – runs over all four oxygen sites in the CuO_4^{5-} center, $\{\dots\}$ is the anticommutator,

$$f(\mathbf{q} \cdot \mathbf{r}) = 2 \sum_{n=0}^{\infty} \frac{(i\mathbf{q} \cdot \mathbf{r})^n}{n!(n+2)} = \sum_{l=0}^{\infty} i^l (2l+1) g_l(qr) P_l(\cos \theta),$$

where $P_l(\cos \theta)$ is the Legendre polynomial, θ being the angle between \mathbf{q} and \mathbf{r} . The functions $g_l(qr)$ are similar to the spherical Bessel functions $j_l(qr)$ which appear in the expansion of $e^{i\mathbf{q}\mathbf{r}}$ (see Ref. [20] for detail).

For nonzero orbital matrix elements we obtain after some routine algebra

$$\langle {}^1A_{1g} | \hat{\Lambda}(\mathbf{q}) | {}^1B_{2g} \rangle = \\ = \frac{gL}{8} (\cos q_x l - \cos q_y l) \langle p_x | \left\{ \hat{l}, f(\mathbf{q} \cdot \mathbf{r}) \right\} | p_y \rangle; \quad (10)$$

$$\langle {}^1A_{1g} | \hat{\Lambda}(\mathbf{q}) | {}^1E_{u,x,y} \rangle = \\ = \pm \frac{igL}{4\sqrt{2}} c_{\pi} \sin q_{y,x} l \langle p_{y,x} | \left\{ \hat{l}, f(\mathbf{q} \cdot \mathbf{r}) \right\} | p_{x,y} \rangle, \quad (11)$$

where $\langle p_x | \left\{ \hat{l}, f(\mathbf{q} \cdot \mathbf{r}) \right\} | p_y \rangle = -\langle p_y | \left\{ \hat{l}, f(\mathbf{q} \cdot \mathbf{r}) \right\} | p_x \rangle$ and

$$\langle p_x | \left\{ \hat{l}_z, f(\mathbf{q} \cdot \mathbf{r}) \right\} | p_y \rangle = \\ = -i [2 \langle g_0(qr) \rangle_{2p} + \langle g_2(qr) \rangle_{2p} (1 - 3e_z^2)]; \quad (12)$$

$$\langle p_x | \left\{ \hat{l}_x, f(\mathbf{q} \cdot \mathbf{r}) \right\} | p_y \rangle = -3i \langle g_2(qr) \rangle_{2p} e_x e_z; \quad (13)$$

$$\langle p_x | \left\{ \hat{l}_y, f(\mathbf{q} \cdot \mathbf{r}) \right\} | p_y \rangle = -3i \langle g_2(qr) \rangle_{2p} e_y e_z. \quad (14)$$

The “+” and “-” signs in (11) are assigned to matrix elements with E_{ux} and E_{uy} , respectively. Thus, the or-

bital vectorial operator $\hat{\Lambda}(\mathbf{q})$ on the basis of the non-ZR multiplet can be replaced by an effective operator as follows:

$$\hat{\Lambda}(\mathbf{q}) = \mathbf{L}_G(\mathbf{q})\hat{G}_z + \overset{\leftrightarrow}{\mathbf{L}}_T(\mathbf{q})\hat{\mathbf{T}}. \quad (15)$$

In contrast with the spin moment the oxygen orbital moment directed perpendicular to the CuO_4 plaquette in the G_z or $T_{x,y}$ modes induces an effective magnetic coupling both with z - and x -, and/or y -components of the neutron spin. In other words, neutrons see the effective orbital magnetic moments to be tilted in $\mathbf{c}^*-\mathbf{q}$ plane. Only for $\mathbf{q} = 0$ $\langle g_0(qr) \rangle_{2p} = 1$, $\langle g_2(qr) \rangle_{2p} = 0$ that is $\mathbf{L}_G \parallel \mathbf{z}$, while for nonzero Bragg vectors such as $\mathbf{q} = (01L)$ or $(10L)$ $\langle g_0(qr) \rangle_{2p}$ and $\langle g_2(qr) \rangle_{2p}$ are of a comparable magnitude [20], that is \mathbf{L}_G can have sizeable xy -plane components. For illustration, in Fig. 3 we

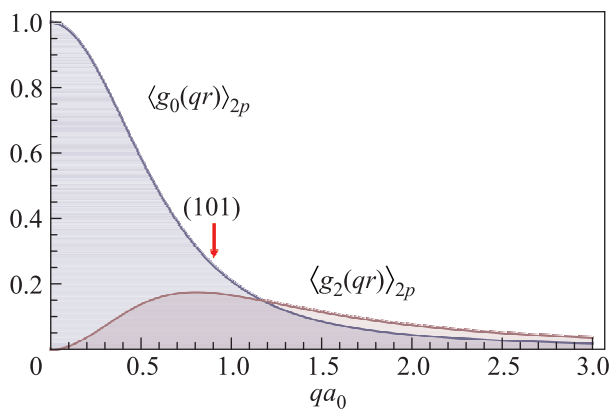


Fig. 3. q -dependence of $\langle g_{0,2}(qr) \rangle_{2p}$ given hydrogenic $2p$ functions (a_0 is Bohr radius). Arrow point to q -value for Bragg vector (101) in $\text{YBa}_2\text{Cu}_3\text{O}_{6+x}$

present the q -dependence of $\langle g_{0,2}(qr) \rangle_{2p}$ given hydrogenic $2p$ functions that clearly supports our message. It is worth noting one more that this seeming tilting depends both on magnitude and direction of neutron scattering vector \mathbf{q} .

We see that the magnetic polarized neutron diffraction measurements provide an unique opportunity to inspect unconventional spin-quadrupole $\langle \hat{\mathbf{V}}\hat{Q}_{xy} \rangle$, spin-dipole $\langle \hat{\mathbf{V}}\hat{d}_{x,y} \rangle$, locally staggered oxygen orbital $\langle \hat{G}_z \rangle$, and oxygen toroidal orbital $\langle \hat{\mathbf{T}} \rangle$ orderings, which are determined by the mixing of the ZR singlet $^1A_{1g}$ with non-ZR terms $^3B_{2g}$, 3E_u , $^1B_{2g}$, 1E_u , respectively. Exps. (5)–(8) and (10)–(14) provide \mathbf{q} -dependence of the formfactors for respective neutron scattering.

All these novel orbital and spin-orbital orders break both the time reversal and tetragonal (Z_4) symmetry, however, our analysis does show that polarized elastic neutron scattering measurements performed at the Bragg scattering wave vectors can detect two hidden

modes which preserve translational symmetry of the lattice, these are the spin-quadrupole $\langle \hat{\mathbf{V}}\hat{Q}_{xy} \rangle$ -mode at $\mathbf{q} = (11L)$ (see Exps. (5) and (7)) or locally staggered orbital G_z -mode at the Bragg vectors such as $\mathbf{q} = (01L)$ or $(10L)$ (see Exps. (10) and (12)–(14)). Namely the latter type of the long range magnetic order has been experimentally observed in the pseudogap phase for three different cuprate families, YBCO, Hg1201 [6], and Bi2212 [8]. Similar short range bidimensional order while occurring at a temperature far below T^* has been observed in LSCO system [6].

Furthermore, to explain the experimental data [6, 8] we do not need to engage the spin-orbital coupling, quantum corrections [2] or orbital currents involving the apical oxygens [4] as the measured polarization effects can be explained with the locally staggered oxygen orbital moments orthogonal to the CuO_2 planes. It is worth noting that the G_z -type ordering preserving the translational symmetry cannot be detected in the polarized elastic neutron scattering measurements performed at the Bragg scattering wave vector such as $\mathbf{q} = (11L)$ that does explain earlier unsuccessful polarized neutron reports [21].

Oxygen orbital moments must inevitably generate local magnetic fields, first of all it concerns a giant ~ 1 T field (given oxygen magnetic moment of $\sim 0.1 \mu_B$) at the oxygen nuclei directed perpendicular to the CuO_2 plane. However, the ^{17}O NMR data on very different cuprates [11] do not reveal signatures of static G_z type mode. At present, there are no published $^{63,65}\text{Cu}$ or ^{17}O NMR studies which give clear results concerning the existence or absence of fields of the predicted magnitude in YBCO, La-214, Hg1201 or Bi2212. The G_z -type orbital magnetic order, as any other moment patterns which have reflection symmetry across the Cu–O–Cu bonds would generate a zero magnetic field on yttrium and barium sites in $\text{YBa}_2\text{Cu}_3\text{O}_{6+\delta}$, $\text{YBa}_2\text{Cu}_4\text{O}_8$, $\text{Y}_2\text{Ba}_4\text{Cu}_7\text{O}_{15-\delta}$, thus making direct ^{89}Y and $^{135,137}\text{Ba}$ NQR/NMR methods as “silent local probes” despite their pronounced sensitivity for weak local magnetic fields. This reconciles the “non-observance” results obtained by ^{89}Y NMR in superconducting $\text{Y}_2\text{Ba}_4\text{Cu}_7\text{O}_{15-\delta}$ and $^{135,137}\text{Ba}$ NQR in superconducting $\text{YBa}_2\text{Cu}_4\text{O}_8$ [12] with neutron scattering results [6]. The ZF- μSR measurements in $\text{YBa}_2\text{Cu}_3\text{O}_{6+\delta}$ and $\text{La}_{2-x}\text{Sr}_x\text{CuO}_4$ [13] have also found no evidence for the onset of magnetic order at the pseudogap temperature T^* . The NMR and μSR experiments clearly rule static G_z type order out. The failure to detect orbital-like magnetic order of the kind observed by spin-polarized neutron diffraction surely indicates that the local fields are rapidly fluctuating outside the μSR or NMR time window or the order is as-

sociated with a small minority phase that evolves with hole doping [13].

Summary. Instead of inactive ZR singlet the ground state of the hole CuO_4^{5-} center should be described by a complex ${}^1A_{1g}$ - ${}^1,3B_{2g}$ - 1,3E_u valent multiplet with several unconventional hidden order parameters such as intra-plaquette's staggered order of Ising-like oxygen orbital magnetic moments or a complex spin-quadrupole ordering. Non-ZR hole centers are believed to be an essential ingredient of both the hole and electron doped cuprates [22]. In particular, these specify many features of the pseudogap regime (see, e.g., Refs. [23, 7]) which indeed manifests clearly seen competing orders. The most convincing evidence of the non-ZR hole centers in cuprates was obtained by experimental findings [6] which provide the first direct evidence of a hidden order incompatible with simple ZR singlet. As we argue, firstly one needs to reconsider the role of oxygen orbitals, especially the in-plane p -orbitals. Indeed, only the competition of the σ and π oxygen holes can explain the emergence of oxygen orbital moments. It is worth noting that the multiplet structure of the ground state makes the hole $[\text{CuO}_4]^{5-}$ centers in cuprates to be the pseudo-Jahn-Teller centers [24]. Thus, the non-ZR hole centers can be responsible for different magnetic and lattice effects which are often addressed to be signatures of the magnetic (spin-fluctuation) or electron-phonon mechanism of the high-temperature superconductivity.

We believe that a large body of puzzling effects governed by the non-ZR structure of the hole centers are secondary ones and are not of primary importance for the high- T_c superconductivity. However, we need to understand these phenomena to understand high- T_c puzzle itself. A full exhaustive explanation of all the cuprate physics governed by the non-ZR hole centers cannot be given at this point, but we propose a consistent picture that can be successfully used for the distinctive and complex description of today and future experimental findings.

The work was partially supported by RFBR grants # 10-02-96032 and 12-02-01039.

-
1. T. M. Rice, K.-Y. Yang, and F. C. Zhang, Rep. Prog. Phys. **75**, 016502 (2012).
 2. C. M. Varma, Phys. Rev. B **55**, 14554 (1997); Nature **468**, 184 (2010).
 3. R. Thomale and M. Greiter, Phys. Rev. B **77**, 094511 (2008).
 4. C. Weber, A. Laeuchli, F. Mila, and T. Giamarchi, Phys. Rev. Lett. **102**, 017005 (2009).

5. A. Kaminski, S. Rosenkranz, H. M. Fretwell et al., Nature (London) **416**, 610 (2002).
6. P. Bourges and Y. Sidis, Comptes Rendus Physique **12**, 461 (2011).
7. J. Xia, E. Schemm, G. Deutscher et al., Phys. Rev. Lett. **100**, 127002 (2008).
8. S. De Almeida-Didry, Y. Sidis, V. Balédent et al., Phys. Rev. B **86**, 020504 (2012).
9. R.-H. He, M. Hashimoto, H. Karapetyan et al., Science **231**, 1579 (2011).
10. N. P. Armitage and J. P. Hu, Phil. Mag. Lett. **84**, 105 (2004); S. V. Borisenko, A. A. Kordyuk, A. Koitzsch et al., Nature **431**, 7004 (2004); M. Lindroos, V. Arpiainen, and A. Bansil, Phys. Rev. Lett. **105**, 189702 (2010).
11. I. Tomeno, T. Machi, K. Tai et al., Phys. Rev. B **49**, 15327 (1994); P. M. Singer, T. Imai, F. C. Chou et al., Phys. Rev. B **72**, 014537 (2005); B. Chen, S. Mukhopadhyay, W. P. Halperin et al., Phys. Rev. B **77**, 052508 (2008); J. Crocker, A. P. Dioguardi, N. Roberts-Warren et al., Phys. Rev. B **84**, 224502 (2011).
12. S. Strässle, J. Roos, M. Mali et al., Phys. Rev. Lett. **101**, 237001 (2008); S. Strässle, B. Graneli, M. Mali et al., Phys. Rev. Lett. **106**, 097003 (2011).
13. G. J. MacDougall, A. A. Aczel, J. P. Carlo et al., Phys. Rev. Lett. **101**, 017001 (2008); J. E. Sonier, V. Pacradouni, S. A. Sabok-Sayr et al., Phys. Rev. Lett. **103**, 167002 (2009); W. Huang, V. Pacradouni, M. P. Kennett et al., Phys. Rev. B **85**, 104527 (2012).
14. F. C. Zhang and T. M. Rice, Phys. Rev. B **37**, 3759 (1988).
15. H. Eskes, L. H. Tjeng, and G. A. Sawatzky, Phys. Rev. B **41**, 288 (1990); H. Kamimura and Y. Suwa, J. Phys. Soc. Jpn. **62**, 3368 (1993).
16. A. S. Moskvin, JETP Lett. **80**, 697 (2004).
17. A. S. Moskvin and Yu. D. Panov, Fiz. Nizk. Temp. (Low Temp. Phys.) **37**, 334 (2011).
18. G. M. De Luca, G. Ghiringhelli, M. Moretti Sala et al., Phys. Rev. B **82**, 214504 (2010).
19. Z. Viskadourakis, I. Radulov, A. P. Petrović et al., Phys. Rev. B **85**, 214502 (2012).
20. G. T. Trammell, Phys. Rev. **92**, 1387 (1953).
21. S.-H. Lee, S. K. Sinha, C. Stassis et al., Phys. Rev. B **60**, 10405 (1999).
22. A. S. Moskvin, Low Temp. Phys. **33**, 234 (2007); Phys. Rev. B **84**, 075116 (2011).
23. C. Panagopoulos, M. Majoros, T. Nishizaki, and H. Iwasaki, Phys. Rev. Lett. **96**, 047002 (2006).
24. A. S. Moskvin and Yu. D. Panov, JETP **84**, 354 (1997); Physica Status Solidi **212**(b), 141 (1999); J. Phys. Chem. Solids **60**, 607 (1999).